University of Groningen

Bachelor's Thesis

# The prospects of HD as a tracer for $H_2$ in interstellar clouds

*Author*
Geart van der Ploeg *(s4160371)*

*Supervisor*
Prof. Dr. Floris van der Tak
*Second reader*
Prof. Dr. John McKean

July 22, 2023

**Abstract**

To study interstellar clouds we need to determine their properties. Their temperatures, particles, densities, sizes, mass, etc. Most of the mass is contained in atomic and molecular hydrogen ($H_2$). Because $H_2$ is invisible in the cold interstellar medium, carbon monoxide (CO) is used to trace $H_2$. In tenuous clouds this is not possible due to the photodissociation of CO. Hydrogen Deuteride (HD) abundances are above 1e-6 compared to the total hydrogen number density $n_H$, at lower cloud densities than CO. We investigate if HD can be observed in interstellar clouds at $n_H = 10^2 - 10^5$. We use a radiative transfer code, RADEX, and data files from LAMDA, to calculate the line flux of HD and CO. Furthermore, we compare the HD line flux to the sensitivity of FIRSST, SPICA, and HERSCHEL, similarly for CO to ALMA. We have found that HD 1-0, 2-1, and 3-2 are observable by the next generation of far infrared space telescopes such as FIRSST. The limits of observing line fluxes above the sensitivity of FIRSST are at $n(H_2) \approx 10cm^{-3}$ for HD 1-0 at 10K, $n(H_2) \approx 150cm^{-3}$ for HD 2-1 at 15K, for T = 30K below $n(H_2) \approx 550cm^{-3}$, $n(H_2) \approx 18cm^{-3}$ for HD 3-2 at 50K. HD 2-1 at 10K and HD 3-2 at 10, 15 K are below the sensitivity of FIRSST. The HD 1-0/2-1 ratio could be used for temperature estimation in diffuse clouds, and in sufficiently warm translucent and dense clouds. The HD 1-0/3-2 and 2-1/3-2 may be used to infer temperature in warm dense molecular clouds.


rijksuniversiteit
groningen

# Contents

# 1 Introduction

When we look at the night sky, we can see countless stars on the celestial sphere. We can study these objects and learn more about their nature. However, we also see stretches of darkness in the space between the stars. Here the interstellar medium (ISM) lies. The stars are much easier to study than the ISM due to the difference in brightness. To study either of these, electromagnetic (EM) radiation can be collected by a telescope equipped with a spectrometer or photodetector to analyze spectra or photon counts. Which are used to infer the intensity at specific wavelengths and the magnitude of stars respectively, see Hanslmeier (2023) for additional details on astronomical instruments and observations. The ISM consists of gas, dust, high-energy particles, and electromagnetic radiation. These are studied by observing emission and absorption lines in spectra, or by using photometric bands (Maciel, 2013).

Diffuse and dark clouds are still challenging to study. The various types of interstellar clouds in the ISM are distinguished by an increase in density. We will see that as we go towards dense clouds, as the name implies, the number density of particles in the cloud will increase. At the same time, the kinetic temperature will decrease, as does the fraction of atomic hydrogen. These clouds are formed from matter in the ISM, which is mainly enriched by supernovae, and asymptotic giant branch (AGB) star winds (Draine, 2011; Wood et al., 1983). However, these clouds are also the stage before star formation. Thus it is important to study interstellar clouds to better understand the complete picture of the gas and dust cycle in the galaxy, see fig. 1.

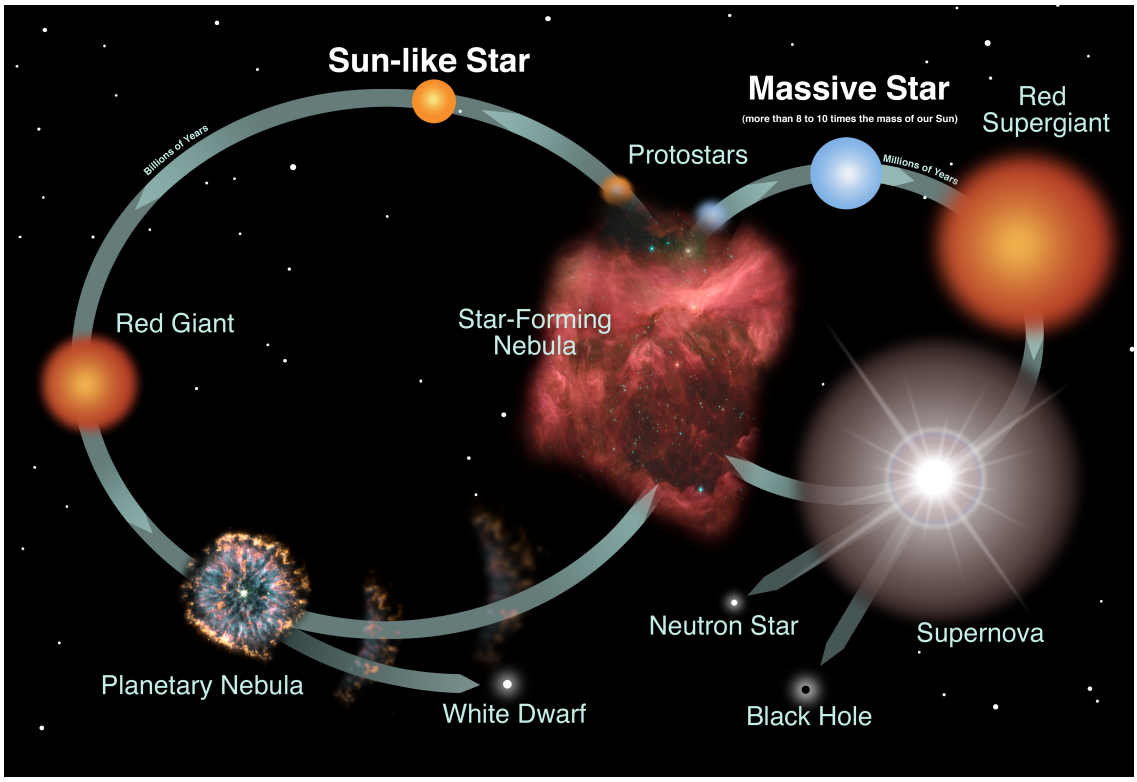


**Figure 1.** Depiction of the lifecycle of stars. We see that sun-like, and massive stars contribute to interstellar clouds which in turn nurse protostars. We also see 'mass end points' such as white dwarfs, neutron stars, and black holes. (Credit: NASA and the Night Sky Network)

To get an idea of how many stars can be formed from an interstellar cloud, we need an estimate of the mass contained in the cloud. Half of the atoms and molecules in the cloud are $H_2$ (Albertsson et al., 2013). By knowing the amount of $H_2$ we can estimate the mass. However $H_2$ is invisible in

cold clouds because the kinetic temperature in the cloud is too low. Togi et al. (2016) provide $510K$ as the lowest permitted quadrupole transition, so the particles in the cloud do not have enough kinetic energy to excite molecular hydrogen. To get an indication of the $H_2$ abundance, carbon monoxide (CO) is used as a tracer. As an example, A survey of the CO 1-0 line, sampling the first and second galactic quadrants has been conducted by the ground based Center for Astrophysics (CfA) 1.2 m telescope to study molecular clouds in the Milky Way (Dame et al., 2001). A tracer is an atom or molecule used to determine quantities that cannot be directly measured. It is determined by using a known relation between the two quantities which holds under certain conditions. In this case, the two quantities are $H_2$ and CO abundances. As mentioned by Glover et al. (2011), the CO abundance mainly depends on photodissociation. More detailed information on CO chemistry and photodissociation can be found in Visser et al. (2009). Photodissociation is the process by which photons destroy molecules. The molecule is excited by a photon through a permitted absorption line, followed by a decay to either vibrationally excited bound levels or unbound levels, the vibrational continuum (Draine, 2011). In the latter case the molecule is destroyed, see fig. 3.

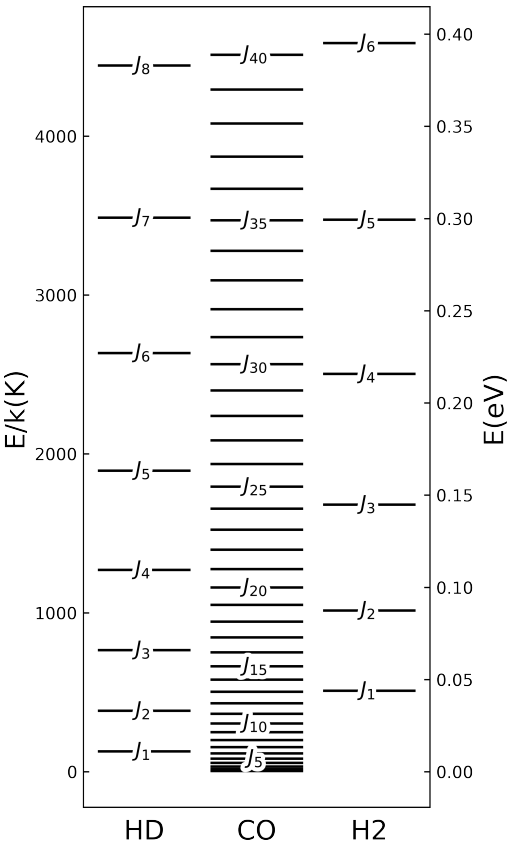


**Figure 2.** The lowest rotational energy levels of HD, CO, $H_2$ in kelvin and electron volt. The energy levels have been labelled by $J_u$, see table 1. $E/k(K) \approx 11605E(eV)$, a rough factor of 10000 between electron volt and kelvin may be used for comparison purposes, e.g. in fig. 3. $H_2$ values from Roueff et al. (2019). HD, CO values from LAMDA

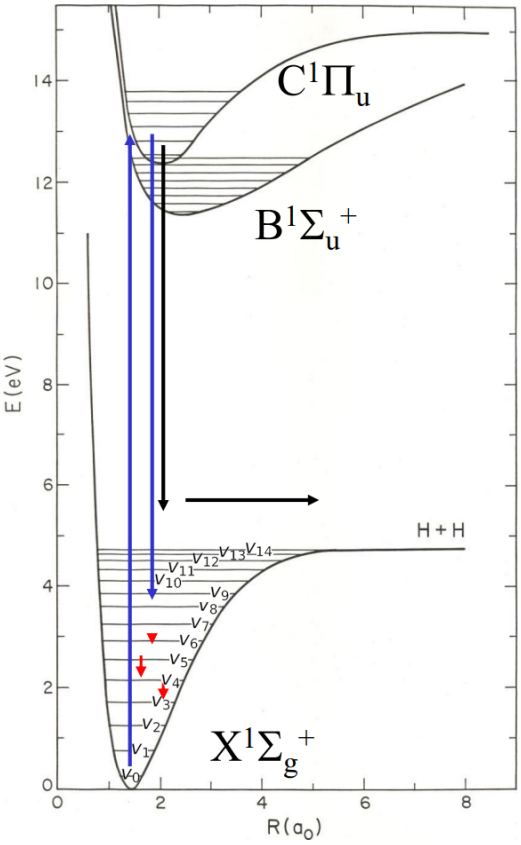


**Figure 3.** The energy as a function of the distance between the molecules, where $a_0$ is the Bohr radius. The vibrational energy levels are labelled by vibrational quantum number $v$ in the ground state X. The red arrows indicate vibrational transitions e.g. $v$ =5-4. The Photodissociation of $H_2$, a photon excites molecule into B and C states after which it decays into the X state, $\approx$ 90% probability. The other $\approx$ 10% decay into the vibrational continuum which leads to dissociation (Dishoeck, 2015)

This means that in diffuse clouds CO is not a reliable tracer for $H_2$. This is why we are going to investigate if Hydrogen Deuteride (HD) can be used as a tracer. We compare the energy levels of HD, CO, and $H_2$ in figs. 2 and 3. We can see that HD and CO require less energy to be excited than $H_2$. The properties we will discuss for the cloud types are kinetic temperature, number density, and visual extinction, $A_V$. The latter is the amount by which an interstellar cloud reduces the brightness of light passing through the cloud due to absorption and scattering of photons, e.g. light from a star behind the cloud in our line of sight (Draine, 2011).

## 1.1 Interstellar Clouds

We now take a look at the various cloud types in the ISM. These will be important in defining where HD is promising.

### 1.1.1 Diffuse Atomic Clouds

As we go up in density from the ISM we first encounter diffuse atomic clouds. These are the most tenuous among the interstellar clouds. With no shielding against the interstellar radiation field, molecules are promptly destroyed due to photodissociation. Therefore, the abundances of molecules are very low. Due to the scarcity of molecules, low densities, and the radiation field, chemistry in these clouds is quite limited. Typical number densities and kinetic temperatures in the cloud are around $10 - 100[cm^{-3}]$ and $100 - 30[K]$ respectively with $A_V \approx 0$ (Snow et al., 2006). The temperature range is inverted as the temperature goes down with increasing density. It should be noted that the defining characteristic of diffuse atomic clouds is the lack of molecules, 90% of the matter should be atomic i.e. the molecular fraction does not exceed 0.1.

### 1.1.2 Diffuse Molecular Clouds

As discussed in the previous subsection, diffuse atomic clouds are not sufficiently shielded against the interstellar radiation field. At the interface of diffuse molecular clouds, there is a shell of diffuse atomic cloud material that shields the diffuse molecular cloud from photodissociation (Roueff et al., 2014). This is the photodissociation region (PDR), see fig. 4. We can see that beyond this region a molecular zone exists. Beyond the PDR, and further into the diffuse molecular cloud, a significant fraction of hydrogen is in the form of molecular hydrogen, $H_2$. Due to the shielding, the radiation field has been attenuated such that the fraction of $H_2$ can exceed 0.1 (Snow et al., 2006). The radiation field is still strong enough to prohibit CO from becoming the dominant form of carbon. Typical number densities and kinetic temperatures are around $100 - 500[cm^{-3}]$ and $100 - 30[K]$ respectively with $A_V \approx 0.2$ (Snow et al., 2006).

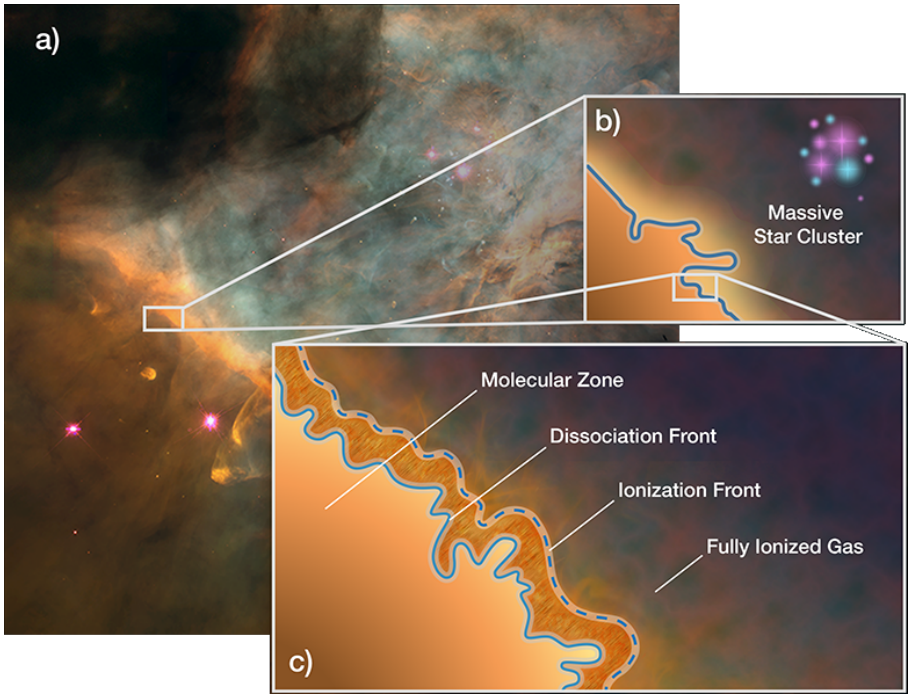


**Figure 4.** An illustration of a photodissociation region within the bar of the Orion Nebula. Panel a is an image from the Hubble Space Telescope Wide Field Planetary Camera 2 (McMaster et al., 2008) The RGB color channels are from nitrogen, hydrogen, and oxygen respectively (NASA et al., 1995). The physical width of panel a is approximately 0.47 parsec. Panels b and c are computer generated. The interface between various cloud regimes can be seen. (Credit: NASA, ESA, CSA, Jason Champion (CNRS), Pam Jeffries (STScI), PDRs4ALL ERS Team)

### 1.1.3 Translucent Clouds

Translucent clouds are a transition between diffuse and dense molecular clouds. They are not well understood and theoretical models are not yet able to agree with all observations regarding atomic and molecular carbon abundances in translucent clouds (Burgh et al., 2010). Similar to diffuse molecular clouds which have a shell, or layer, of diffuse atomic cloud material, so are translucent clouds surrounded by diffuse molecular material. Typical number densities and kinetic temperatures are around $500 - 5000?[cm^{-3}]$ and $50? - 15[K]$ respectively with $A_V \approx 1 - 2$. As indicated by the question mark in the ranges, the upper limits of the density and temperature are quite uncertain. For a detailed review of diffuse atomic, diffuse molecular, and translucent clouds we refer to Snow et al. (2006).

### 1.1.4 Dense Molecular Clouds

When almost all carbon is molecular, i.e. the molecular carbon fraction approaches one, we go from translucent clouds to finding ourselves in dense molecular clouds. As with the previous types of cloud, dense molecular clouds too, are enveloped by the material of the previous cloud type which offers shielding from photodissociation. The protection against energetic radiation, i.e. X-ray (Odaka et al., 2011), UV (Yamamoto, 2017), causes molecules to be abundant and electron abundances to be very low. Electrons are still present due to processes such as cosmic-ray ionization. When the dense molecular cloud becomes sufficiently dense and cold, CO abundances start to drop due to freeze-out (Pagani et al., 2012). This is the process where species are captured by dust grains in cold clouds (Hocuk et al., 2014). Typical number densities and kinetic temperatures are around $10^4 - 10^5[cm^{-3}]$ and $50 - 10[K]$ respectively with $A_V \approx 5 - 10$. For a detailed review of dense molecular clouds or cold dark clouds, we refer to Bergin et al. (2007).

## 1.2 HD

HD abundances increase sooner, i.e in more diffuse clouds than CO. Le Petit et al. (2002) show that the photodissociation rate of HD rapidly decreases from $A_V \approx 0.2$ and is at a rate less than $10^{-15}(s^{-1})$ by the time $A_V \geq 1$. The former extinction is associated with diffuse molecular clouds and the latter with translucent clouds. Snow et al. (2006) show that the CO abundance only becomes significant in the translucent cloud regime, see fig. 5. We expect that HD will perform the best in diffuse molecular clouds.

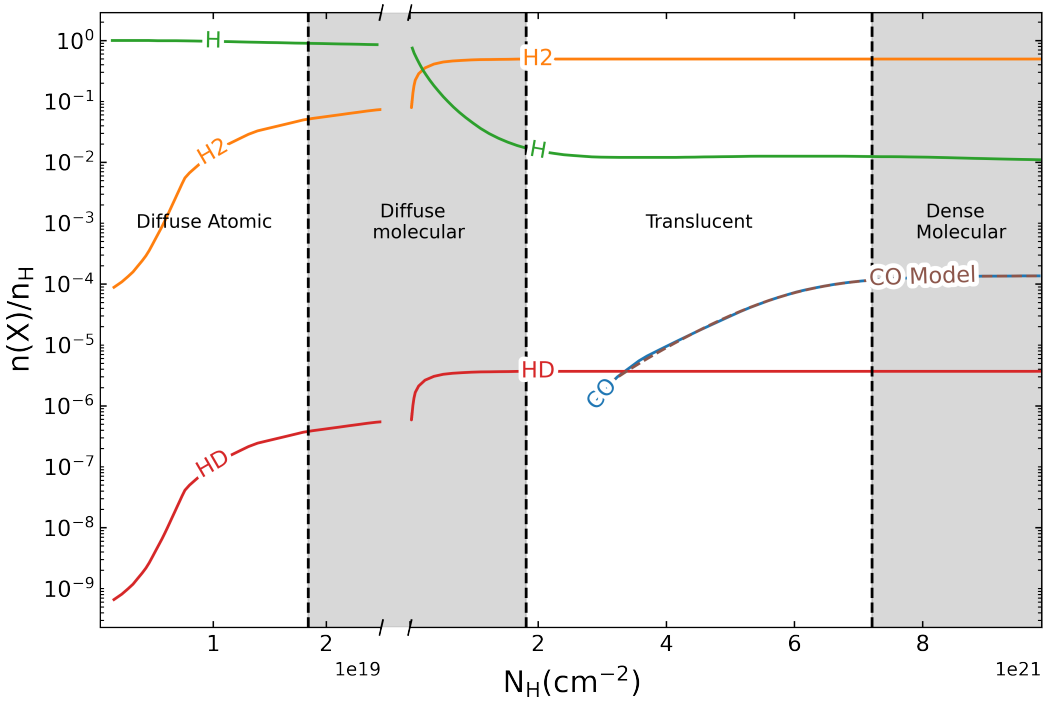


**Figure 5.** Atom and molecule number densities as a fraction of hydrogen number density plotted against hydrogen column density (Snow et al., 2006). The lines for H, $H_2$, HD, CO, and the CO model are labeled with their names.

## 1.3 Thesis outline

In this thesis, we look at HD as a candidate for tracing $H_2$. We start by determining if the emission lines of HD are strong enough to be observed. We use a radiative transfer model to simulate the emission lines and compare the predicted flux intensities from HD and CO. We then determine which lines can be observed and if we can use these lines to determine the cloud mass and temperature. We finalize by presenting our conclusion and possibilities for future work.

# 2 Methods

Based on photodissociation alone, HD seems like a good candidate. However, the wavelengths of the HD line emissions, see table 1, are in the range of $15 - 112\mu m$, to which the atmosphere is opaque. HD has to be observed from space, though currently there are no instruments in space that can observe at the wavelengths of HD. This is a disadvantage compared to CO. However, this will not always be the case as the FIRSST probe is planned to launch in 2035 to observe wavelengths between $2.8 - 588\mu m$ (Meixner et al., 2019). We compare Herschel to FIRSST and SPICA, see table 3. Herschel was a space telescope active from 2009 - 2013, observing in wavelengths from $55-671\mu m$ Pilbratt et al., 2010. SPICA was a candidate for ESA's fifth medium class mission with observable wavelengths from $10 - 420\mu m$ (Team, 2021). Herschel and SPICA provide a reference of which line fluxes are observable with FIRSST.

**Table 1.** Molecular lines used in our model, data from the Leiden Atomic and Molecular Database (LAMDA) (Schöier et al., 2005)

| | | **HD** | | | **CO** | | |
|---|---|---|---|---|---|---|---|
| $J_u$ | $J_l$ | $\nu$ **(GHz)** | $\lambda$ $[\mu m]$ | **E_u/k [K]** | $\nu$ **(GHz)** | $\lambda$ $[\mu m]$ | **E_u/k [K]** |
| 1 | 0 | 2675 | 112 | 128 | 115 | 2600 | 6 |
| 2 | 1 | 5332 | 56 | 384 | 231 | 1300 | 17 |
| 3 | 2 | 7952 | 38 | 766 | 346 | 870 | 33 |
| 4 | 3 | 10518 | 29 | 1271 | 461 | 650 | 55 |
| 5 | 4 | 13015 | 23 | 1895 | 576 | 520 | 83 |
| 6 | 5 | 15429 | 19 | 2636 | 691 | 430 | 116 |
| 7 | 6 | 17746 | 17 | 3487 | 807 | 370 | 155 |
| 8 | 7 | 19957 | 15 | 4445 | 922 | 330 | 199 |

We investigate the first eight lines of HD, due to the availability of data for these transitions in LAMDA (Schöier et al., 2005). These radiative transitions have upper total angular momentum quantum number $J_u$ from 2 through 9. All of these transitions fall within the wavelength range of FIRSST so we investigate their fluxes. We also include the first 8 transitions of CO to compare their fluxes.

## 2.1 Calculating Line Fluxes

To determine which lines can be observed we use RADEX, developed by van der Tak et al. (2007), to calculate the line intensities at a combination of cloud parameters. RADEX includes background radiation, e.g. the cosmic microwave background (CMB), optical depth effect, and collisional and radiative processes in the calculation. To run these calculations we need to provide the HD and CO molecular data files from LAMDA, the column densities of these molecules, the number density of the collision partner $H_2$, the background radiation is taken to be the CMB at $T = 2.73K$. Lastly, we provide the kinetic temperature of the cloud, we will investigate the line fluxes at $10, 15, 30, 50,$ and $100K$. We choose these kinetic temperatures such that we have three kinetic temperatures for every cloud type, diffuse, translucent, and dense. Two kinetic temperatures at the extremes of the cloud type, i.e. the minimum and maximum temperature, and one that is roughly in between these values, see table 2. We obtain our calculated size in the table by taking the quotient of the column density and number density. Now that we have qualified the parameters we need, we are going to quantify them. The process of quantifying the input parameters for RADEX is shown in the following diagram:

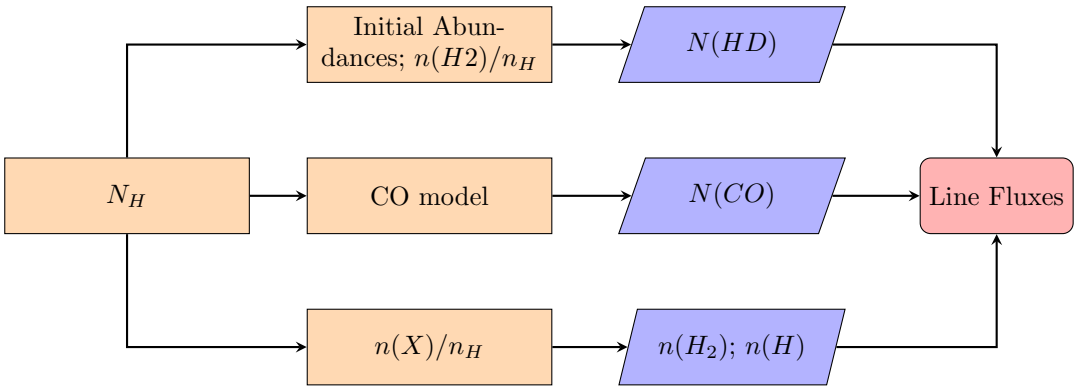


**Figure 6.** Summary of obtaining our parameters, we use the third column as parameters for our calculations with RADEX to get our line fluxes.

We will continue by introducing the notation of column and number densities after which we will clarify the diagram.

### 2.1.1 Definitions of Column and Number Densities

The column density refers to the total amount of matter along a line of sight through a medium, in our case interstellar clouds. It is the number of particles in an area perpendicular to the line of sight. We refer to the column density of a particle by $N_X$ or $N(X)$ where $X$ refers to the specific particle, e.g. $H_2$. The first notation $N_X$ is the total column density including atoms of species X in any atom or molecule. The second notation $N(X)$ refers to the column density of species X in that form only. The column density provides information about the chemical and physical properties of the cloud such as composition and densities (Mangum et al., 2015; Mangum et al., 2017). In a similar manner to the column density, the number density is referred to as $n_X$ or $n(X)$. Again, $n_X$ refers to the number density of species X in any atom or molecule, whereas $n_X$ refers to the number density of species X in that form only.

### 2.1.2 Adopted Parameters for our Calculations

We begin with the abundances of H, $H_2$, CO, and HD relative to $n_H = n(H) + 2n(H_2)$. These quantities are a function of the column density $N_H = N(H) + 2N(H_2)$ as seen in fig. 5. Additionally, we know that $N_H$ at the borders of the cloud types in fig. 5 correspond to the densities in units of $cm^{-3}$ in table 2, i.e. 100, 500, and $10^4$. We use an upper limit for the dense molecular clouds density of $10^5(cm^{-3})$ in our calculations. This value is in line with the upper mean density of dense cloud cores from Bergin et al. (2007). We choose the number of samples M, and interpolate our relative abundances, $n(X)/n_H$, from the lower bound of diffuse molecular clouds to the upper bound of dense molecular clouds, i.e. from $N_H \approx 2 \cdot 10^{19} - 10^{22}(cm^{-2})$. With our interpolated values we can add a line for $n(HD)/n_H$ to fig. 5. We use the HD and $H_2$ abundance with respect to $n_H$ from Albertsson et al. (2013). These quantities are respectively $1.5 \cdot 10^{-5}$ and 0.499. We multiply $n(H2)/n_H$ by the former and divide by the latter resulting in $n(HD)/n_H = n(H_2)/n_H \cdot 1.5 \cdot 10^{-5}/0.499$. We use the relative abundance of $H_2$ since the self-shielding of HD is very similar to $H_2$ at $T = 200K$ (Wolcott-Green et al., 2011). We continue by fitting a sigmoid to the CO curve of fig. 5, see fig. 7.

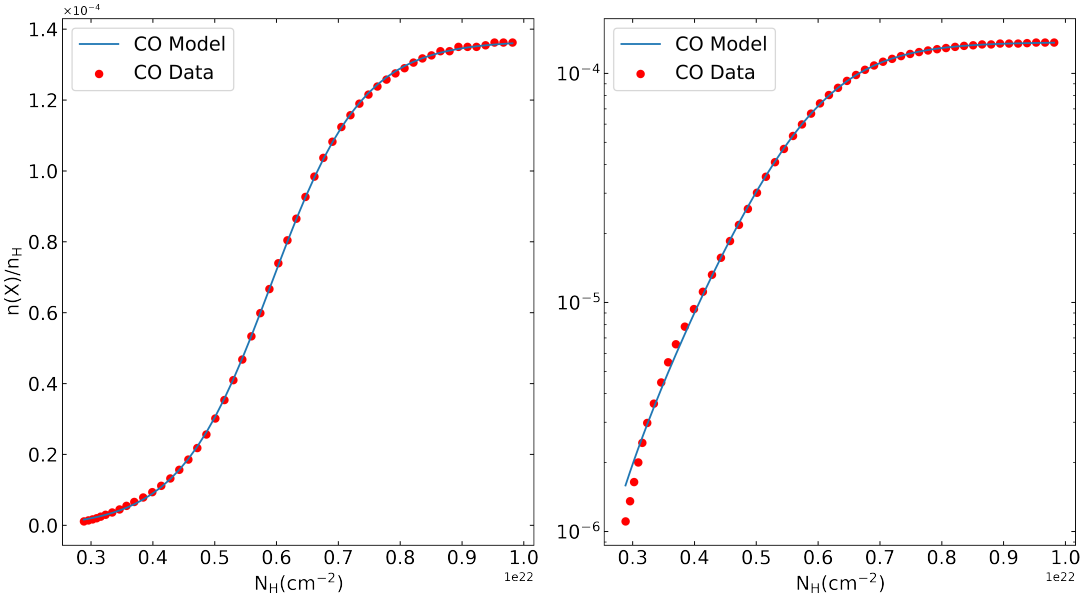


**Figure 7.** Fit of $n(CO)/n_H$ as a function of $n_H$, data from Snow et al. (2006). The left panel shows the fit in linear space revealing the sigmoid curve nature. The right panel shows the fit in semi-log space.

We now use our data and model to calculate $N(X)$ for HD and CO from $n(X)/n_H$ by using the following relation: $N(X) = n(X)/n_H \cdot N_H$. This gives us the column densities we need for our calculations. see fig. 8. This figure shows that HD is present in diffuse molecular clouds while CO is negligible, which agrees with the trend we see in fig. 5.

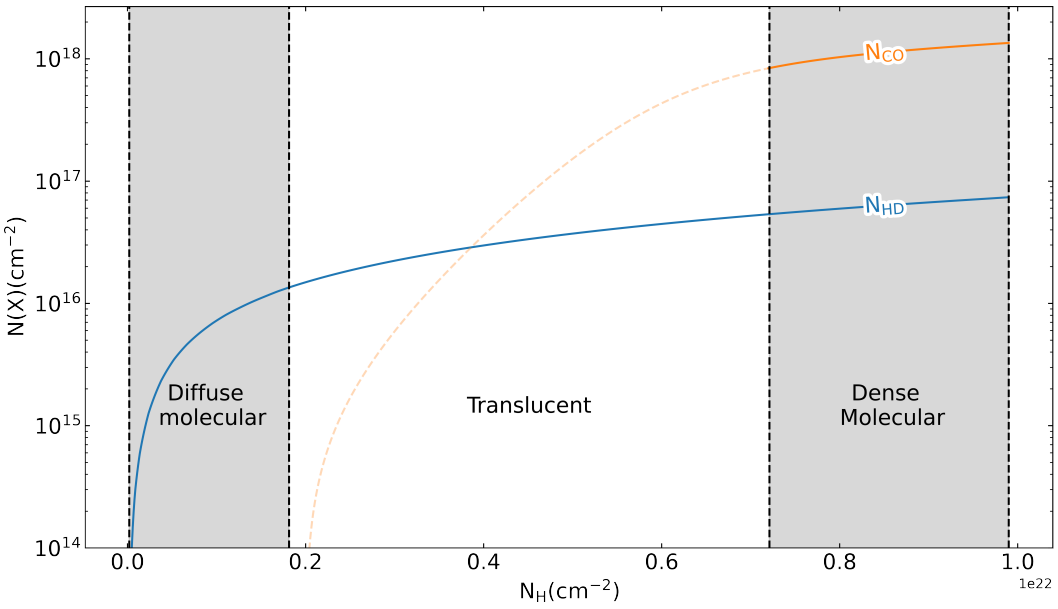


**Figure 8.** HD and CO column density as a function of hydrogen column density. The short dashed part of $N_{CO}$ is made transparent because we are not interested in translucent clouds. The lines go through regions denoting the type of cloud the hydrogen column density corresponds to.

We continue by deriving the number densities for the collision partners of HD and CO, $H_2$, and H.

We use our interpolated column densities $N_H$, and the values for $n_H$ and $N_H$ at the borders of the regimes, 100, 500, $10^4$, $10^{-5}(cm^{-3})$, and $1.84{\cdot}10^{19}$, $1.82{\cdot}10^{21}$, $7.2{\cdot}10^{21}$, $9.9{\cdot}10^{21}(cm^{-2})$ respectively. Interpolating $N_H$ for these given $n_H$ and $N_H$ gives our interpolated $n_H$. We multiply the latter with $n(X)/n_H$ to obtain $n(H_2)$ and $n(H)$. Lastly, we define the temperature of background radiation to $2.73(K)$, similar to the CMB.

**Table 2.** Cloud properties

| | **Diffuse Molecular** | **Translucent** | **Dense Molecular** |
|---|---|---|---|
| $n_H(cm^{-3})$ | 100 - 500 | 500 - $10^4$ | $> 10^4$ |
| T $[K]$ | 30 - 100 | 15 - 50 | 10 - 30 |
| $N_H(cm^{-2})$ | (1.8 - 180]) $\cdot 10^{19}$ | (1.8 - 7.2) $\cdot 10^{21}$ | (7.2 - 9.9)$\cdot 10^{21}$ |
| $size(pc)^{a,g}$ | 0.06 - 1.18 | 0.23 - 1.18 | $>$ 0.03 - 0.32 |
| $size(pc)^h$ | $> 0.01^b$ | 0.08 - $0.6^c$, $<1^d$ | 0.03 - $15^e$ |
| $Mass(M_\odot)^{a,f}$ | (0.03 - 1064)$\cdot 10^{-2}$ | 0.08 - 213 | $>$ (3.5 - 4276)$\cdot 10^{-3}$ |

[a]: Dependent on $n_H$, $N_H$ from this table;[b]: Black et al., 1991;[c]: Only one cloud, dependant on distance (Thiel et al., 2019);[d]: Noterdaeme et al., 2010;[e]: Bergin et al., 2007; Lang, 1978;[f]: The mass is calculated by assuming a spherical cloud geometry;[g]: These are the sizes of the clouds in our model;[h]: These are sizes from observations found in literature.

## 2.2 Improving Calculation Speed

Now that we have the $H_2$ number density, the HD and CO column densities, and the kinetic temperatures, we can calculate the line fluxes by providing our parameters along with the molecular data files to RADEX. Some of the properties in these files can be found in table 1. To speed up our calculations we call RADEX through the pool function from Python's multiprocessing package. We use HD to compare the speed of these calculations. To quantify the time our calculations take we use the packages tqdm to measure the iterations per second, and cProfile to find time costly parts in our code to improve iteration time. Our unmodified code starts at 21.53 iterations per second averaging from 2500 iterations. We now implement the pool function and improve the handling of our input and output files. Compared to our initial calculation rate, this speeds up the code by a factor of $\approx 26.32$. We now check the speed improvements solely from implementing the pool function, this speeds up the code by a factor of $\approx 2.93$ based on 10201 calculations for both before and after implementing the pool function. For our HD line flux calculations, we reach an average of 566.65 iterations per second.

## 2.3 Telescopes of Interest

Once the simulated line fluxes are obtained from our simulations in RADEX, we compare these fluxes to the sensitivity of various telescopes: Herschel, SPICA, and FIRSST see table 3. We note that SPICA is no longer a candidate for the M5 mission[1] and is therefore discontinued. To make this comparison we use the $5\sigma$ sensitivity in one hour to determine if the lines can be observed.

[1] https://sci.esa.int/s/AplJM2A

**Table 3.** Selected telescopes and their instruments.

| **Telescope / Instrument** | **Wavelengths** $[\mu m]$ | **Representative Sensitivity** $5\sigma$ **in 1 hr** $[erg \cdot cm^{-2}s^{-1}]$ | **Year** |
|---|---|---|---|
| AKARI[a] | 2 - 180 | 1.7E-10 | 2006 |
| Herschel[b] | 55 - 671 | - | 2009 |
| PACS[b] | 55 - 210 | 1.3E-13 | |
| SPICA[c] | 10 - 420 | - | (2030)[d] |
| SAFARI | 34 - 230 | 8.8E-17 | |
| High Resolution Fourier Transform Spectrometer | 34 - 230 | 1.9E-16 | |
| FIRSST[e] | 2.8 - 588 | - | 2035[f] |
| Grating | 25 - 588 | 3.7E-18 | |
| High Resolution | 25 - 588 | 7.4E-18 | |
| Ultra high resolution | 100 - 200 | 2.8E-16 | |
| ALMA band 2[g] | 2600 – 4500 | 2.3e-17 | 2011 |

[a]: AKARI (Murakami et al., 2007);[b]: Herschel Space Observatory, Photodetector Array Camera and Spectrometer (PACS) (Pilbratt et al., 2010);[c]: SPace Infrared telescope for Cosmology and Astrophysics (SPICA) (Team, 2021);[d]: SPICA has been discontinued;[e]: Far InfraRed Spectroscopy Space Telescope (FIRSST), previously Origins Space Telescope (Meixner et al., 2019);[f]: FIRSST is planned to launch in 2035 if it is selected;[g]: Bolatto et al., 2015.

# 3 Results

We now present the calculated line fluxes for the adopted parameters. We begin by comparing the HD 1-0 line to the CO 1-0 line fig. 9. In this figure, we also compare the fluxes to the 1-hour $5\sigma$ sensitivities of Herschel, SPICA, and FIRSST. This line indicates which flux would be $5\sigma$ above the signal-to-noise ratio after one hour of exposure. We continue by comparing HD 1-0 to HD 2-1 and HD 3-2, see figs. 10 and 11.

## 3.1 Line Fluxes

Our first calculations of the line fluxes compare the HD and CO 1-0 lines fig. 9. We have calculated line fluxes at 10, 15, 30, 50 and $100K$ for the molecular hydrogen number density $n(H_2)$ between the lower bound in diffuse clouds and upper bound in dense clouds as discussed in section 2.1.2. In this figure, we can see that dense clouds have higher line flux than diffuse clouds. Furthermore, the HD 1-0 line fluxes are above the FIRSST sensitivity for $n(H_2) \leq 10$. In the region $10cm^{-3} \leq n(H_2) \leq 180cm^{-3}$ the HD 1-0 line flux is higher than the CO 1-0 line flux. The sharp drop in CO 1-0 flux around $n(H_2) = 60cm^{-3}$ is propagated from our CO model fig. 7 through or column densities fig. 8 to our line fluxes.

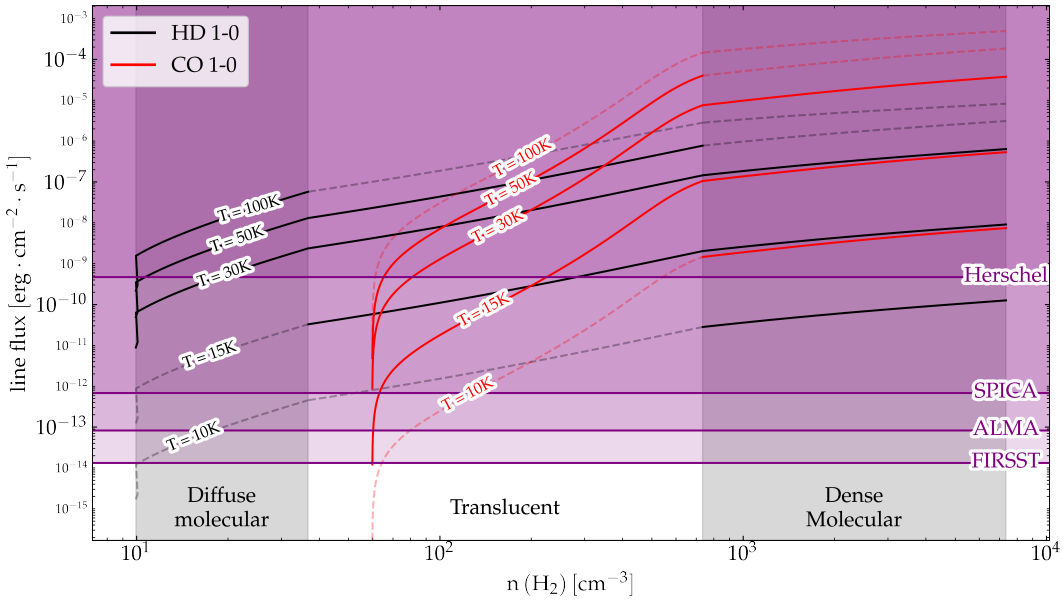


**Figure 9.** Line flux for HD 1-0, CO 1-0, at various temperatures as a function of $H_2$ column density. The HD and CO lines are separated into short dashed and full lines. The former indicates that the temperature used to simulate the line fluxes is not within the cloud regime, the latter indicates the opposite. The telescope lines for Herschel, SPICA, and FIRSST are the sensitivity $5\sigma$ in one hour. The shaded regions above these lines indicate that the line fluxes are observable within one hour at $5\sigma$.

In figures figs. 10 and 11 that our line fluxes drop with every successive transition i.e. the line flux for HD 1-0 > HD 2-1 > HD 3-2. However, there is also an increase in slope, which can be seen especially in the shaded region for dense clouds in figs. 10 and 11. The slopes differ so the ratios between the line fluxes will not be constant. This means the line flux ratios can be used to trace the gas. Not all of the temperature lines are above the FIRSST sensitivity line. The HD 2-1 line in T=15k translucent cloud material is observable from $n(H_2) \gtrapprox 150$ in 1 hour at $5\sigma$. The HD 3-2 line in T=30k translucent cloud material is observable from $n(H_2) \gtrapprox 500$ in 1 hour at $5\sigma$. The HD 3-2 line in T=50k diffuse molecular cloud material is observable from $n(H_2) \gtrapprox 18$ in 1 hour at $5\sigma$. The lines HD 2-1 in 10K cloud material, and HD 3-2 in 10, 15K cloud material are

far below the sensitivity line and not observable. Similarly for the other transitions of HD, with $J_u > 4$, listed in table 1, the line fluxes were too low to observe, their figures have been omitted.

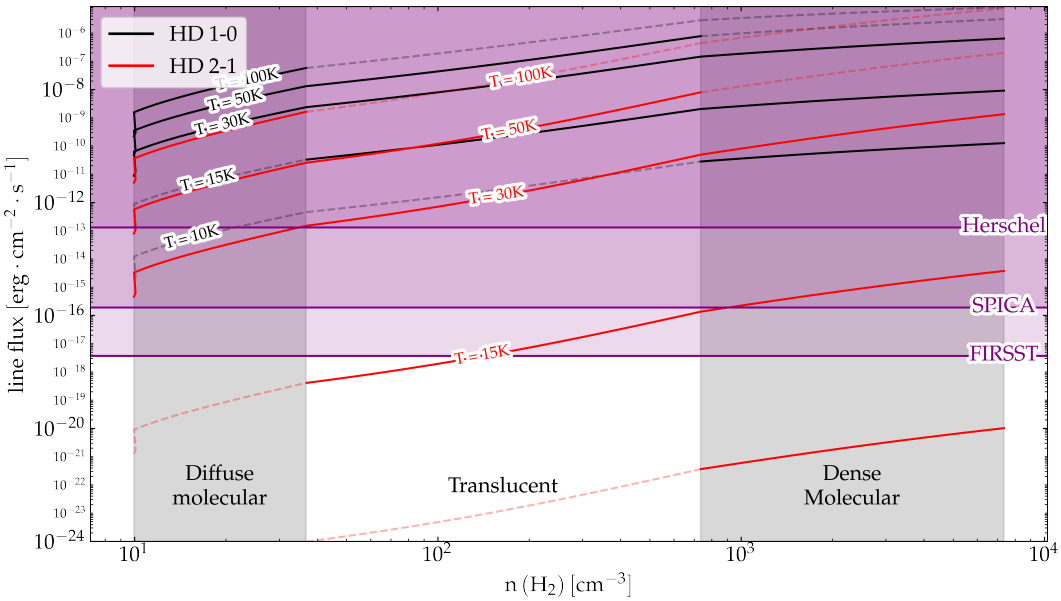


**Figure 10.** Line flux for HD 1-0, HD 2-1, at various temperatures as a function of $H_2$ column density. See fig. 9 for an extensive description of the layout. The lowest HD 2-1 line is unlabelled, this is the 10K line.

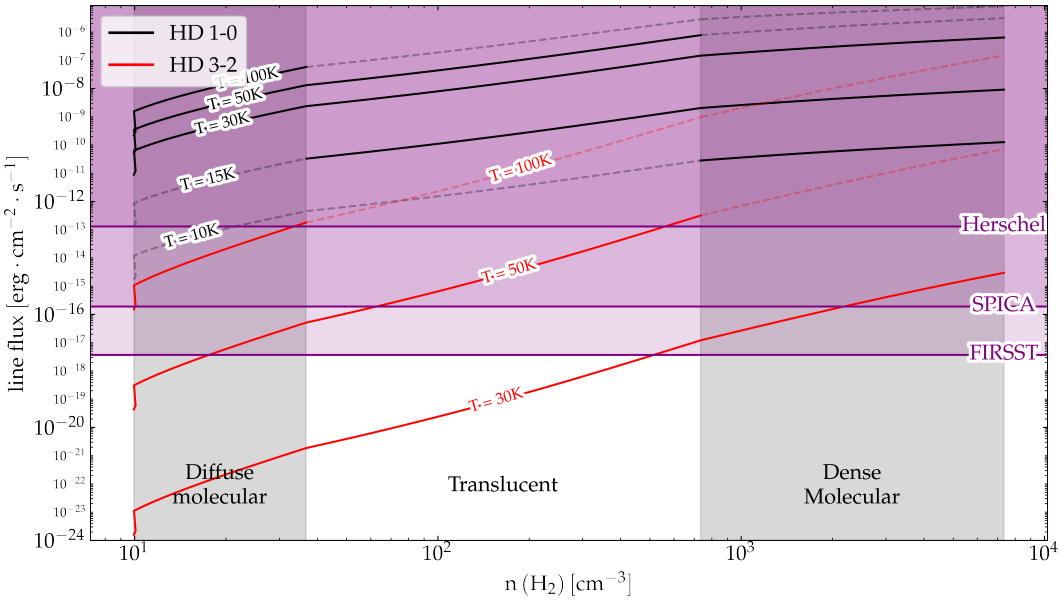


**Figure 11.** Line flux for HD 1-0, HD 3-2, at various temperatures as a function of $H_2$ column density. See fig. 9 for an extensive description of the layout.

## 3.2 Required Exposure Time

Now that we know which lines can be observed under which temperatures and molecular hydrogen number densities, we calculate how much exposure time we need. This is computed by,

$[Flux(5\sigma, 1hr)/(meanlineflux)]^2$. This is the square of the quotient of the one hour $5\sigma$ flux by the mean line flux of a temperature line in one cloud type, table 4. The result is the exposure time required for the line fluxes to be $5\sigma$ above the signal-to-noise ratio. We calculate the required exposure time for every line in our calculations, i.e. HD 1-0, 2-1, and 3-2, and for every kinetic temperature corresponding to the cloud type, e.g. 30, 50, and 100 K for diffuse molecular clouds table 4. We can see that except for the HD 3-2 line at 30K, the line flux of a diffuse cloud with average $n(H_2)$ is observable in one hour at $5\sigma$.

**Table 4.** The mean flux and mean observation time found for our calculated line fluxes for HD 1-0, 2-1, and 3-2 using the grating of FIRSST. The bold numbers in the second part of our table show line fluxes that are observable within one hour at $5\sigma$. It should be noted that the HD 3-2 line at 30K in translucent cloud material requires an exposure time of $\approx$ 5760 seconds, which is only $\approx$ 30% more than one hour.

| **Line/Flux**[a] | **Diffuse Molecular** | | | **Translucent** | | | **Dense Molecular** | | |
|---|---|---|---|---|---|---|---|---|---|
| | **30K** | **50K** | **100K** | **15K** | **30K** | **50K** | **10K** | **15K** | **30K** |
| 1-0 | 9.5e-10 | 5.2e-09 | 2.3e-08 | 8.4e-10 | 6.0e-08 | 3.2e-07 | 8.6e-11 | 6.2e-09 | 4.4e-07 |
| 2-1 | 5.7e-14 | 9.7e-12 | 6.1e-10 | 4.3e-17 | 1.6e-11 | 2.5e-09 | 4.9e-21 | 1.8e-15 | 6.4e-10 |
| 3-2 | 5.5e-22 | 1.5e-17 | 5.4e-14 | 5.1e-61 | 2.9e-18 | 7.7e-14 | 5.1e-61 | 5.1e-61 | 1.0e-15 |
| | **Time(hr)** | | | | | | | | |
| 1-0 | **1.6e-17** | **5.3e-19** | **2.7e-20** | **1.9e-17** | **3.8e-21** | **1.3e-22** | **1.8e-15** | **3.5e-19** | **7.1e-23** |
| 2-1 | **4.5e-09** | **1.5e-13** | **3.8e-17** | **7.5e-03** | **5.7e-14** | **2.1e-18** | 5.6e+05 | **4.1e-06** | **3.2e-17** |
| 3-2 | 4.5e+07 | **5.9e-02** | **4.8e-09** | 5.2e+85 | 1.6e+00 | **2.3e-09** | 5.2e+85 | 5.2e+85 | 1.2e-05 |

[a]: The line flux is in units of $erg \cdot cm^{-2} \cdot s^{-1}$.

## 3.3 Line Flux Ratios

We now use our line fluxes to investigate if their ratios can give information on the clouds. We show the three possible ratios from our observable lines in fig. 12. The red lines are the contours of the observable ratios at $5\sigma$ sensitivity. Any measurements above this line are observable. The HD 1-0 / 2-1 ratio shows promise for dense molecular clouds for log line ratios up to around 8. For diffuse molecular clouds, we can use the HD 1-0 / 2-1 ratios. For translucent and dense clouds, the log line ratio looks indicative of temperature. The HD 1-0 / 3-2 and 2-1 / 3-2 line ratios are only usable for warm dense molecular clouds $T \approx 30K$, and for translucent clouds around $T \gtrsim 30K$.

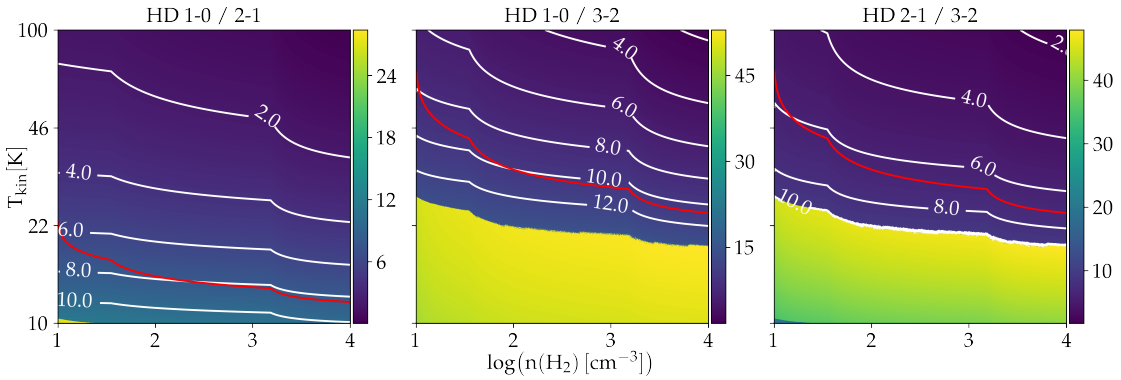


**Figure 12.** Calculated HD line ratios. In the left pane, we see the ratio HD 1-0 / 2-1, in the middle pane HD 1-0 / 3-2, and in the right pane HD 2-1 / 3-2. The color bar indicates the difference between the transitions in orders of magnitude. We see these ratios as a function of $H_2$ number density in $cm^{-3}$, and kinetic temperature in $K$. The white lines are contours at constant line ratios. The red contours are the observable ratios at $5\sigma$ in one hour. Any measurement above the red lines is observable.

# 4 Discussion

To trace the masses of diffuse and dense $H_2$ clouds we calculated the line fluxes of HD and compared these with CO fig. 9. We then investigated if these fluxes are above the sensitivity of $5\sigma$ in one hour of Herschel, SPICA, and FIRSST, for CO we compare to ALMA, see figs. 10 and 11. We continued by determining at which temperatures the HD lines are detectable with FIRSST table 4. Lastly, we identified which line ratios are observable fig. 12.

In our comparison between HD and CO, we find that the line fluxes increase with cloud density. The line fluxes may be overestimated in dense cloud regions because the data is based on a PDR model without taking CO and HD depletion from freeze-out into account. This influences the column densities we derive from fig. 5. CO freezes out onto dust at $n_{H_2} \gtrsim 3 \cdot 10^5 cm^{-3}$ (Whitworth et al., 2018). Additionally, Caux et al. (2002) suggest that CO depletes before HD. In the models from Sipilä et al. (2013), HD depletes at a density of $n_H = 2 \cdot 10^6 cm^{-3}$ on time scales of $10^5$ years in starless cores. Therefore, including the proper formation and destruction channels of HD and CO in our calculations will improve our line flux comparison.

All the line fluxes are above the FIRSST $5\sigma$ sensitivity in one hour for HD 1-0, 2-1, 3-2 at T = 10, 15, 30, 50, 100 K except for the following line fluxes: HD 1-0 dips below the sensitivity line at the lowest value of our molecular hydrogen number densities, $n(H_2) \approx 10 cm^{-3}$. HD 2-1 is below the sensitivity line for T = 10K, and for T = 15K below $n(H_2) \approx 150 cm^{-3}$. HD 3-2 is below the sensitivity line for T = 10, 15 K, for T = 30K below $n(H_2) \approx 550 cm^{-3}$, and for T = 50K below $n(H_2) \approx 18 cm^{-3}$. Studying these lines with space telescopes that are currently planned, FIRSST or similar, will be time-consuming.

The exposure time required for the line fluxes for every line in our calculations, i.e. HD 1-0, 2-1, and 3-2, and for every kinetic temperature corresponding to the cloud type, e.g. 30, 50, and 100 K for diffuse molecular clouds table 4 show us that the HD 1-0 line is completely observable at the sensitivity of FIRSST. This implies that we can find column densities of HD by observing with FIRSST. Diffuse clouds are the best suited for studying using HD compared to translucent and dense clouds because the required observation times almost all fall above the sensitivity line of FIRSST.

From the 3-2 line and onward, the line flux is not observable in diffuse clouds, the line flux ratio between HD 1-0, 2-1 is the only ratio we can use to infer cloud properties. However, large values for $dT_{kin}/dlog(n_(H_2))$ of HD 1-0/2-1 in diffuse molecular clouds could result in a less precise estimate of kinetic temperature. A relation with uncertainties can be derived from future research. Still, the HD 1-0/2-1 ratio looks promising for determining the temperature in diffuse molecular clouds, and may also be used to this end in translucent and dense molecular clouds. Though over the $n(H_2)$ range for these two cloud types, $dT_{kin}/dlog(n_(H_2))$ varies more than for diffuse clouds, this can cause a less precise temperature estimate. The HD 1-0 / 3-2 and 2-1 / 3-2 line ratios are only usable for warm dense molecular clouds $T \approx 30K$, and for translucent clouds around $T \gtrsim 30K$.

# 5 Conclusion and Future Work

We have found that HD 1-0, 2-1, and 3-2 are observable by the next generation of far infra red space telescopes such as FIRSST. The limits of observing line fluxes above the sensitivity of FIRSST are at $n(H_2) \approx 10cm^{-3}$ for HD 1-0 at 10K, $n(H_2) \approx 150cm^{-3}$ for HD 2-1 at 15K, for T = 30K below $n(H_2) \approx 550cm^{-3}$, $n(H_2) \approx 18cm^{-3}$ for HD 3-2 at 50K. HD 2-1 at 10K and HD 3-2 at 10, 15 K are below the sensitivity of FIRSST. The HD measurements will be useful, because the line ratios look promising as a tracer for kinetic temperature. We note that the HD 1-0/2-1 ratio could be used for temperature estimation in diffuse clouds. Also in translucent dense clouds, if they are not too cold. The HD 1-0 / 3-2 and 2-1 / 3-2 may be used to infer temperature in warm dense molecular clouds due to the low line fluxes in diffuse and translucent clouds of HD 3-2. In the future, calculations can indicate at which temperatures and number densities the line fluxes are resolvable, i.e. above the sensitivity line of FIRSST, for the diffuse, translucent and dense clouds. We already plotted this for $n(H2)$ in fig. 12. These values could be used to determine from which temperatures the HD 1-0, 2-1, and 3-2 lines are observable in diffuse, translucent and dense clouds. The adopted parameter values can be improved by considering important formation and destruction channels of HD. For dense clouds, freeze-out models should be included to simulate how much the column density and line flux drop. Once freeze-out is included we can investigate dense molecular clouds at higher densities. The models can be made more realistic by including more molecules.

$H_2$ and H have been included as collision partners. Additionally, we can use more collision partners for HD: He, $H^+$, and electrons. RADEX uses the thermal ortho/para ratio if not specified for $\mathrm{p}-\mathrm{H}_2$ and $\mathrm{o}-\mathrm{H}_2$, this ratio changes during the lifetime of a cloud (Pagani et al., 2011). The line ratios can be used to determine the temperature, we have plotted this in fig. 12.

## Acknowledgements

I would like to thank Prof. Dr. Floris van der Tak for his guidance and support throughout this research. During our meetings and email exchanges, he provided many useful insights and feedback. I am very grateful to the creators of the computer program RADEX and the data files from LAMDA. This research would not have been possible without their public availability. I would also like to thank my peers for lending an ear and engaging in discussion on the topic. And finally, I would like to thank my friends and family for their support and encouragement.

# References


Albertsson, T., D. A. Semenov, A. I. Vasyunin, T. Henning, and E. Herbst (Aug. 2013). "New Extended Deuterium Fractionation Model: Assessment at Dense ISM Conditions and Sensitivity Analysis". In: ApJS 207.2, 27, p. 27. arXiv: 1110.2644 [astro-ph.SR].

Bergin, E. A. and M. Tafalla (Sept. 2007). "Cold Dark Clouds: The Initial Conditions for Star Formation". In: ARA&A 45.1, pp. 339–396.

Black, J. H. and E. F. van Dishoeck (Jan. 1991). "Chemistry and Small-Scale Structure of Diffuse and Translucent Clouds". In: *Fragmentation of Molecular Clouds and Star Formation*. Ed. by E. Falgarone, F. Boulanger, and G. Duvert. Vol. 147, p. 139.

Bolatto, A. D., J. Carpenter, S. Casassus, et al. (2015). *ASAC recommendations for ALMA 2030*. Tech. rep. European Southern Observatory.

Burgh, E. B., K. France, and E. B. Jenkins (Jan. 2010). "Atomic and Molecular Carbon as a Tracer of Translucent Clouds". In: ApJ 708.1, pp. 334–341. arXiv: 0911.1812 [astro-ph.GA].

Caux, E., C. Ceccarelli, L. Pagani, S. Maret, A. Castets, and J. R. Pardo (Feb. 2002). "HD 112 mu m in absorption and extreme CO depletion in a cold molecular cloud". In: A&A 383, pp. L9–L13.

Dame, T. M., D. Hartmann, and P. Thaddeus (Feb. 2001). "The Milky Way in Molecular Clouds: A New Complete CO Survey". In: ApJ 547.2, pp. 792–813. arXiv: astro-ph/0009217 [astro-ph].

Dishoeck, E. F. van (2015). *Photodissociation in Astrophysics*. Presentation. Obtained from: https://home.strw.leidenuniv.nl/~ewine/photo/workshops/2015-02/collected_presentations/Leiden2015_photo.pdf. Leiden Observatory/MPE.

Draine, B. T. (2011). *Physics of the Interstellar and Intergalactic Medium*.

Glover, S. C. O. and M. .-. Mac Low (Mar. 2011). "On the relationship between molecular hydrogen and carbon monoxide abundances in molecular clouds". In: MNRAS 412.1, pp. 337–350. arXiv: 1003.1340 [astro-ph.GA].

Hanslmeier, A. (2023). *Introduction to Astronomy and Astrophysics*.

Hocuk, S., S. Cazaux, and M. Spaans (Feb. 2014). "The impact of freeze-out on collapsing molecular clouds". In: MNRAS 438.1, pp. L56–L60. arXiv: 1310.8466 [astro-ph.SR].

Lang, K. R. (Oct. 1978). "Small Dense Molecular Clouds which Envelope Groups of T-Tauri Stars (Paper presesnted at the Conference on Protostars and Planets, held at the Planetary Science Institute, University of Arizona, Tucson, Arizona, between January 3 and 7, 1978.)" In: *Moon and Planets* 19.2, pp. 185–198.

Le Petit, F., E. Roueff, and J. Le Bourlot (July 2002). "D/HD transition in Photon Dominated Regions (PDR)". In: A&A 390, pp. 369–381.

Maciel, W. J. (2013). *Astrophysics of the Interstellar Medium*.

Mangum, J. G. and Y. L. Shirley (Mar. 2015). "How to Calculate Molecular Column Density". In: PASP 127.949, p. 266.

— (June 2017). *Corrigendum: How to Calculate Molecular Column Density*. Publications of the Astronomical Society of the Pacific, Volume 129, Issue 976, pp. 069201 (2017).

McMaster, M. and et al. (2008). *Wide Field and Planetary Camera 2 Instrument Handbook v. 10.0*.

Meixner, M., A. Cooray, D. Leisawitz, et al. (2019). *Origins Space Telescope Mission Concept Study Report*. arXiv: 1912.06213 [astro-ph.IM].

Murakami, H., H. Baba, P. Barthel, et al. (Oct. 2007). "The Infrared Astronomical Mission AKARI*". In: PASJ 59, S369–S376. arXiv: 0708.1796 [astro-ph].

NASA O'Dell, C. and S. Wong (1995). "Crucible of Creation: Panoramic Image of Center of the Orion Nebula". In: *HubbleSite*. Accessed: July 12, 2023.

Noterdaeme, P., P. Petitjean, C. Ledoux, S. López, R. Srianand, and S. D. Vergani (Nov. 2010). "A translucent interstellar cloud at z = 2.69. CO, $H_2$, and HD in the line-of-sight to SDSS J123714.60+064759.5". In: A&A 523, A80, A80. arXiv: 1008.0637 [astro-ph.CO].

Odaka, H., F. Aharonian, S. Watanabe, Y. Tanaka, D. Khangulyan, and T. Takahashi (Oct. 2011). "X-Ray Diagnostics of Giant Molecular Clouds in the Galactic Center Region and Past Activity of Sgr A*". In: ApJ 740.2, 103, p. 103. arXiv: 1110.1936 [astro-ph.GA].

Pagani, L., A. Bourgoin, and F. Lique (Dec. 2012). "A method to measure CO and $N_2$ depletion profiles inside prestellar cores". In: A&A 548, L4, p. L4.

Pagani, L., E. Roueff, and P. Lesaffre (Oct. 2011). "Ortho-$H_2$ and the Age of Interstellar Dark Clouds". In: ApJ 739.2, L35, p. L35. arXiv: 1109.6495 [astro-ph.GA].

Pilbratt, G. L., J. R. Riedinger, T. Passvogel, et al. (July 2010). "Herschel Space Observatory. An ESA facility for far-infrared and submillimetre astronomy". In: A&A 518, L1, p. L1. arXiv: 1005.5331 [astro-ph.IM].

Roueff, E., H. Abgrall, P. Czachorowski, K. Pachucki, M. Puchalski, and J. Komasa (Oct. 2019). "The full infrared spectrum of molecular hydrogen". In: A&A 630, A58, A58. arXiv: 1909.11585 [physics.atom-ph].

Roueff, E., M. Ruaud, F. Le Petit, B. Godard, and J. Le Bourlot (Feb. 2014). "Diffuse Cloud Models: Successes and Challenges". In: *The Diffuse Interstellar Bands*. Ed. by J. Cami and N. L. J. Cox. Vol. 297, pp. 311–320.

Schöier, F. L., F. F. S. van der Tak, E. F. van Dishoeck, and J. H. Black (Mar. 2005). "An atomic and molecular database for analysis of submillimetre line observations". In: A&A 432.1, pp. 369–379. arXiv: astro-ph/0411110 [astro-ph].

Sipilä, O., P. Caselli, and J. Harju (June 2013). "HD depletion in starless cores". In: A&A 554, A92, A92. arXiv: 1304.4031 [astro-ph.GA].

Snow, T. P. and B. J. McCall (Sept. 2006). "Diffuse Atomic and Molecular Clouds". In: ARA&A 44.1, pp. 367–414.

Team, S. S. (July 2021). *SPICA MISSION STUDY SUMMARY REPORT*. Tech. rep. ESA-SPI-EST-MIS-RP-001. Publication date: 12 July 2021. European Space Agency, p. 106.

Thiel, V., A. Belloche, K. M. Menten, et al. (Mar. 2019). "Small-scale physical and chemical structure of diffuse and translucent molecular clouds along the line of sight to Sgr B2". In: A&A 623, A68, A68. arXiv: 1901.03231 [astro-ph.GA].

Togi, A. and J. D. T. Smith (Oct. 2016). "Lighting the Dark Molecular Gas: $H_2$ as a Direct Tracer". In: ApJ 830.1, 18, p. 18. arXiv: 1607.08036 [astro-ph.GA].

van der Tak, F. F. S., J. H. Black, F. L. Schöier, D. J. Jansen, and E. F. van Dishoeck (June 2007). "A computer program for fast non-LTE analysis of interstellar line spectra. With diagnostic plots to interpret observed line intensity ratios". In: A&A 468.2, pp. 627–635. arXiv: 0704.0155 [astro-ph].

Visser, R., E. F. van Dishoeck, and J. H. Black (Aug. 2009). "The photodissociation and chemistry of CO isotopologues: applications to interstellar clouds and circumstellar disks". In: A&A 503.2, pp. 323–343. arXiv: 0906.3699 [astro-ph.GA].

Whitworth, A. P. and S. E. Jaffa (Mar. 2018). "A simple approach to CO cooling in molecular clouds". In: A&A 611, A20, A20. arXiv: 1811.06814 [astro-ph.GA].

Wolcott-Green, J. and Z. Haiman (Apr. 2011). "Suppression of HD cooling in protogalactic gas clouds by Lyman-Werner radiation". In: MNRAS 412.4, pp. 2603–2616. arXiv: 1009.1087 [astro-ph.CO].

Wood, P. R., M. S. Bessell, and M. W. Fox (Sept. 1983). "Long-period variables in the Magellanic Clouds : Supergiants, AGB stars, Supernova precursors, Planetary nebula precursors, and enrichment of the interstellar medium." In: ApJ 272, pp. 99–115.

Yamamoto, S. (2017). "Chemistry of Molecular Clouds I: Gas Phase Processes". In: *Introduction to Astrochemistry: Chemical Evolution from Interstellar Clouds to Star and Planet Formation*. Tokyo: Springer Japan, pp. 91–130. ISBN: 978-4-431-54171-4.